Spatial variability of organic carbon storage and sources in China's subtropical *Halophila beccarii* seagrass meadow

Xiaomei Shen

shenxm@gzhu.edu.cn

Guangzhou University

Yiguo Hong

Guangzhou University https://orcid.org/0000-0002-6255-4100

Fei Ye

Guangzhou University

Jiapeng Wu

Guangzhou University

Yu Wang

Guangzhou University

Fen Guo

Hang Wan

Hongbin Liu

Hong Kong University of Science and Technology https://orcid.org/0000-0002-3184-2898

Article

Keywords:

Posted Date: September 3rd, 2025

DOI: https://doi.org/10.21203/rs.3.rs-7456384/v1

Additional Declarations: There is **NO** Competing Interest.

Abstract

Seagrass meadows are crucial in marine blue carbon storage. However, blue carbon storage of seagrass meadows in subtropical regions dominated by small-sized species may be overestimated, and the primary factors regulating organic carbon (C_{org}) variability remain uncertain. Here we investigated spatial patterns in blue carbon storage and sediment C_{org} sources in China's subtropical estuarine meadows of the small seagrass, *Halophila beccarii*, and identified key environmental drivers influencing its spatial heterogeneity. The results revealed that these species may store less blue carbon than estimated, with low carbon stocks revealed in China's estuarine meadows. Sediment carbon varied spatially, influenced by moisture, salinity, $CaCO_3$, and bulk density. Terrigenous sources contributed most sediment carbon, followed by seagrass, and phytoplankton, exhibiting distinct spatial variation along the transect. These findings highlight the need for refined blue carbon assessments in subtropical regions and suggest managing environmental factors to enhance seagrass carbon storage as a climate solution.

1. Introduction

The increasing emission of greenhouse gases, particularly CO_2, has driven global warming to critical levels, with the global monthly mean CO_2 concentration reaching 427 ppm in 2025[1]. This alarming trend highlights the urgency of addressing one of the most unrelenting global environmental challenges. In this context, quantifying the carbon sequestration capacity of natural ecosystems has emerged as a key strategy for mitigating atmospheric CO_2 levels and combating climate change[2,3]. The concept of "blue carbon" was formally introduced in 2009 through a landmark report by the United Nations Environment Programme (UNEP), highlighting the critical role of marine ecosystems in global carbon cycling. Seagrass ecosystems represent one of the most efficient carbon sinks within marine environments and global carbon pools[4,5,6]. Despite occupying less than 0.2% of the ocean's area (approximately 330,000 km² globally), seagrass meadows store an estimated 19.9 Pg of organic carbon (C_{org}), accounting for 10–18% of the total oceanic carbon burial[7]. The remarkable carbon sequestration capacity of seagrass meadows originates from three key mechanisms: (1) high primary productivity, (2) efficient particle trapping by seagrass canopies, and (3) slow organic matter decomposition in underlying anaerobic sediments. Importantly, over 90% of this blue carbon is stored in sediments[8,9], making sediment C_{org} pools the dominant component of seagrass carbon stocks.

Research on seagrass meadows as blue carbon sinks originated in the 1980s, when Smith (1981)[10] first identified the significant carbon sequestration potential of marine macrophytes. Subsequent studies have systematically quantified blue carbon storage across global seagrass ecosystems. Comprehensive analysis by Fourqurean et al. (2012)[7] revealed substantial regional variation, with sediment carbon stocks ranging from 23.6 Mg C ha^{-1} in Indo-Pacific meadows to 372.4 Mg C ha^{-1} in Mediterranean systems. Their global synthesis established mean carbon stocks of 2.52 ± 0.48 Mg C ha^{-1} in living biomass and 194.2 Mg C ha^{-1} in sediments (0–1 m depth). Notably, Fourqurean et al. (2012)[7] standardised sediment sampling to 1 m depth, as this surface layer represents the most labile carbon

pool susceptible to mineralisation. Although recent studies have enhanced spatial resolution of blue carbon storage data[9,11,12,13,14,15], global estimates of seagrass C_{org} stocks remain largely derived from limited field sampling. This is particularly evident in West Pacific subtropical monsoon regions, where data gaps continue to hinder the integration of seagrass meadows into policy frameworks such as carbon finance mechanisms and international climate agreements[16].

Existing research has demonstrated significant spatial variation in seagrass carbon stocks, occurring both regionally and locally. This variability complicates stock assessments, as shown by *Posidonia oceanica* meadows, where 2 m depth sites contain 14–16 times more carbon than 32 m depth sites[17]. Similarly, along Kalimantan Island's coastal gradient, sediment carbon stocks (0–1 m depth) demonstrate substantial spatial variation, with values increasing from 80.37 Mg C ha^{-1} in near-shore zones to 121.84 and 243.33 Mg C ha^{-1} in mid- and far-shore zones, respectively[18]. Ricart et al. (2020)[19] documented a pronounced estuarine gradient in Port Curtis, Australia, where C_{org} stocks decreased from 52.16 mg cm^{-3} in upper estuary meadows to 1.06 mg cm^{-3} at the estuary mouth, reflecting landscape-driven variations in sediment dynamics and allochthonous carbon inputs. Similarly, in China's Liusha Bay, Shen et al. (2024)[9] reported C_{org} stocks ranging 39.74 to 157.12 Mg ha^{-1}, with maximum values occurring near deep-water channels in far-shore zones. Even within the same species, significant regional differences exist—*Zostera marina* meadows store 23.1 Mg ha^{-1} in Baltic Sea sediments versus 351.7 Mg ha^{-1} (15× higher) in Mediterranean systems[20]. While seagrasses provide critical carbon sequestration services, small-bodied species like *Halophila beccarii* (33.9 ± 7.7 Mg ha^{-1} in Zanzibar)[21] remain understudied due to their diminutive morphology and restricted intertidal distributions[22].

Spatial variability of C_{org} stocks in seagrass meadows is influenced by multiple interacting environmental factors[23,24]. Key drivers include: (1) seagrass species composition and coverage[25]; (2) hydrodynamic conditions[26,27]; (3) sediment properties (e.g., particle size, often mediated by hydrodynamics)[28,29]; (4) climate zone[30]; (5) carbon sources proximity[31]; (6) biogeochemical processes[32]; and (7) landscape configuration (e.g., patchy vs. continuous beds)[31, 33]. However, the relative importance of these factors in driving blue carbon variability remains poorly understood, particularly for specific seagrass meadows.

While seagrasses are widely recognized as important carbon sinks, site-specific studies are required to elucidate the influence of local environmental conditions on C_{org} stocks across spatial scales[34]. High-resolution assessments of blue carbon stocks are critical for improving multi-scale carbon accounting[35]. Hence, this study aims to: (1) quantify C_{org} storage in intertidal *Halophila beccarii* (*H. beccarii*) meadows of the Yifengxi Estuary, southern China; (2) identify the key drivers of spatial variability in C_{org} stocks; and (3) characterise sources of sediment C_{org}. As a comprehensive assessment of C_{org} storage and sources in subtropical *H. beccarii* meadows of the Yifengxi Estuary, the study findings will enhance the accuracy of blue carbon accounting and inform conservation strategies for seagrass meadows in the Pacific subtropical monsoon region.

2. Materials and methods

2.1 Study area and sampling methods

The study was conducted in the Yifengxi seagrass meadow (418 ha), located in the subtropical monsoon-influenced Yifengxi Estuary of Shantou City, southern China (116°53'-116°56'E, 23°31'-23°33'N; Fig. 1). This area represents the largest seagrass meadow in eastern Guangdong Province and the most extensive *Halophila beccarii* habitat in the region[36,37]. The area experiences an annual mean temperature of 21.9°C and receives 1098 mm of precipitation, predominantly between May and September. Notably, *H. beccarii* is ecologically significant as: (1) one of the only two extant seagrass species considered evolutionarily ancient and (2) one of ten seagrass species globally classified as vulnerable (VL) on the International Union for Conservation of Nature (IUCN) Red List[38], highlighting its conservation priority.

Field surveys and sample collection were conducted during spring tide low tides from April 12–17, 2022. Seven transects were systematically distributed across the meadow to ensure representative coverage of the seagrass habitat. At each transect, 2–3 replicate quadrats were established (0.5 m × 0.5 m) and spaced at ≥ 50 m apart (Fig. 1). In-situ water quality parameters were recorded (temperature, pH, conductivity, and dissolved oxygen) using a calibrated multi-parameter meter (YSI 30M-25; YSI, Yellow Springs, OH, USA).

A total of 16 living plant samples and 20 sediment cores were collected across the seven established transects (Supplementary Table 1). Three plant samples were collected from each of transects Y1 through Y5, and a single sample from transect Y6. Due to challenging silty substrate conditions that necessitated boat access during high tide periods, no plant samples were collected from transect Y7. Plant sampling was conducted using a 10 cm diameter PVC corer cautiously inserted vertically to a depth of 20 cm to ensure complete capture of both above- and below-ground biomass components. Samples were placed in pre-labelled monofilament mesh transport bags immediately after collection to maintain sample integrity during transfer from field to laboratory.

In the laboratory, plant samples underwent a standardized processing protocol. First, residual sediments were removed through sequential washing, beginning with seawater rinses in the field followed by additional freshwater rinses under controlled laboratory conditions. Epiphytes were then gently removed from leaf surfaces using soft plastic scrapers to avoid tissue damage, after which shoot density was recorded for each sample. The cleaned samples were subsequently separated into their constituent above-ground (leaves and stems) and below-ground (rhizomes and roots) components. Each component was individually wrapped in acid-washed aluminium foil and stored at 4°C to preserve sample integrity until further analysis, following established protocols[39].

Sediment cores were systematically collected from the upper 1 m profile using a Russian Peat Corer (1 m length, 0.07 m sector radius) to minimise compaction during sampling. Three replicate cores were obtained at each of transects Y1–Y5 and Y7, while two cores were collected at transect Y6 (Table 1).

Surface litter layer and any living biomass were removed to ensure clean sediment sampling. Following extraction, each intact core was immediately sectioned into seven depth intervals (0–10, 10–20, 20–30, 30–40, 40–50, 50–70, and 70–100 cm) in the field. From each stratified subsample, a 15 mL vertical aliquot was collected using a sterile 20 mL syringe for detailed analysis. The remaining sediment from each depth interval was placed in pre-labelled, self-sealing bags. All samples were immediately cryopreserved using dry ice in the field and maintained frozen during transport to the laboratory for subsequent analysis. This stratified sampling approach allowed for comprehensive characterisation of sediment properties and carbon distribution throughout the entire 1 m profile while preserving the vertical integrity of each core segment.

2.2 Seagrass traits, sediment characteristics, and C_{org} stock measurements

For each sampling quadrat, key morphological characteristics of *H. beccarii*, including leaf length, leaf width, and shoot height, were measured from five randomly selected shoots using digital callipers with 0.1 mm precision. The plants were then carefully separated into above-ground (stem, leaf sheath, and leaf) and below-ground (root and rhizome) components after the measurements. All plant tissues were oven-dried at 60°C for 72 hours until constant weight was achieved to determine dry biomass. C_{org} stocks in living seagrass biomass were calculated using the following approach: first, above- and below-ground biomass values (g m^{-2}) were multiplied by the standardized carbon conversion factor of 0.34[40]. These values were then scaled to per hectare units (Mg C ha^{-1}). Total living biomass carbon stocks were derived by summing carbon stocks across all sampling regions, weighted by their respective spatial coverage[9,39,41].

The 140 sediment subsamples were oven-dried at 60°C until constant weight was achieved. Moisture content and dry bulk density (DBD) were measured and calculated. C_{org} content was measured using an elemental analyzer (Vario EL , Germany). The C_{org} density (mg cm^{-3}) in each sediment layer was calculated by multiplying C_{org} content by the corresponding DBD (g cm^{-3}) using Eq. (1).

$$\mathrm{C_{org}\ density} = \mathrm{DBD} \times \mathrm{C_{org}} \times 1000$$

1

where DBD is the dry bulk density of the sediment subsample (g cm^{-3}) and C_{org} is the organic carbon content (g/g). Sediment C_{org} stocks per layer were calculated by multiplying C_{org} density by layer thickness (10, 20, or 30 cm). The total stock for the upper 1 m was derived by summing all layers (Mg C ha^{-1}). Total blue carbon storage (Mg C ha^{-1}) comprised of sediment and living biomass C_{org} stocks[9,39,41]. The g C cm^{-2} was converted to the standard Mg C ha^{-1} using the following: 1 Mg = 10^6 g; 1 ha = 10^9 cm^2.

The dried subsamples were ground and sieved (100-mesh). To remove inorganic carbon, the samples were treated with 1 mol L^{-1} HCl for 24 h. For salinity analysis, a 5:1 water-to-sediment extract was stirred (30 min), filtered, and measured using an HQ4300 meter (Hach, Loveland, CO, USA). For pH, 2.5:1 extracts were stirred (10 min), settled (1–3 h), and analysed using the HQ4300 meter. Organic matter and carbonate (CO_3^{2-}) contents were measured using the sequential loss on ignition (LOI) method, with furnacing steps at 550°C and 950°C, respectively[41,42]. Organic matter content was calculated as per Eq. 2:

$$\%\mathrm{LOI}_{550} = \frac{(\mathrm{m}_0\text{-}\mathrm{m}_1) \times 100}{\mathrm{m}_0}$$

2

where $\%LOI_{550}$ is the organic matter content, m_0 (g) is the initial dry weight, and m_1 (g) is the remaining weight after 550°C furnacing. The CO_3^{2-} in sediments typically exists as carbonate ($CaCO_3$)[41]. $CaCO_3$ content in sediments was calculated as per Eq. 3:

$$\%\mathrm{LOI}_{950} = \frac{(\mathrm{m}_1\text{-}\mathrm{m}_2) \times 100}{\mathrm{m}_0}$$

3

where m_0 (g) is the initial dry weight, m_1 (g) is the remaining weight after furnacing at 550°C, and m_2 (g) is the remaining weight after furnacing at 950°C. The weight loss at 950°C (LOI) was multiplied by 1.36 estimated CO_3^{2-} content, based on molecular weights of CO_2 (44 g mol^{-1}) and carbonate (60 g mol^{-1})[42,43]. A linear regression ($\%LOI_{550}$ vs. $\%C_{org}$) was established using Eq. (4).

$$\%\mathrm{C}_{\mathrm{org}} = \mathrm{a} \times \%\mathrm{LOI}_{550}\text{-}\mathrm{b}$$

4

where $\%C_{org}$ is the organic carbon content, $\%LOI_{550}$ is the organic matter content, and fitted coefficients, *a* and *b*, were determined from the measured values of $\%C_{org}$ and %LOI, respectively.

2.3 Determination for stable carbon isotopic compositions and C_{org} sources

To quantify the relative contributions of different C_{org} sources to sediment C_{org} in the estuarine seagrass meadows, three potential end-members were considered: terrigenous, seagrass-derived, and phytoplankton organic matter. The proportional contributions of these sources were estimated based on their stable carbon isotope ($\delta^{13}C$) signatures using the Bayesian mixing model MixSIAR[44]. The $\delta^{13}C$ end-member values were established as follows: *H. beccarii* seagrass (-21.767‰) and phytoplankton (-20.000‰) values were obtained from Kennedy et al. (2010)[45], while the terrigenous organic matter signature (-28.640‰) was determined by integrating data from global terrigenous organic matter and

seasonal measurements of suspended organic matter from 20 reservoirs in Guangdong Province[45,46]. For $\delta^{13}C$ analysis, air-dried sediment subsamples were finely ground using an agate mortar and pestle, and measured by an elemental analyzer-isotope ratio mass spectrometry system (EA-IRMS; Manufacturer, City, Abb. State, Country), with values reported in per mil (‰) relative to the Vienna Pee Dee Belemnite (V-PDB) standard.

2.4 Statistical analysis method

We conducted comprehensive statistical analyses to examine patterns in the carbon storage data. All datasets were rigorously evaluated for normality and variance homogeneity before the analysis using Shapiro–Wilk and Levene's tests, respectively. Appropriate data transformations, including log10 for strictly positive values and log10(x + 1) for datasets containing zeros, were applied when parametric assumptions were not met. For normally distributed data, one-way analysis of variance (ANOVA) was performed, followed by Dunn's post-hoc pairwise comparisons, with statistical significance set at $p < 0.05$. Correlation analyses, principal component analysis (PCA), and linear fitting were conducted to identify key drivers of C_{org} variability and explore multivariate relationships among environmental factors and carbon stocks. All parametric tests and regression analyses were performed using SPSS Statistics 27 (IBM Corp., Armonk, NY, USA), while multivariate analyses were implemented in R version 4.3.3.

3. Results

3.1 Environmental conditions, seagrass characteristics, and C_{org} stocks

Environmental conditions and seagrass characteristics were monitored in the *H. beccarii* meadow at Yifengxi Estuary. During the study period, water temperature averaged 23 ± 2.03°C, with dissolved oxygen (7.11 ± 1.09 mg L^{-1}), pH (8.02 ± 0.33), and salinity (5.55 ± 1.36‰) recorded. The meadow occurred in shallow waters (0.1–0.5 m depth) with variable seagrass coverage (45–85%). Morphometric measurements revealed average leaf dimensions of 8.37 ± 1.82 mm (length) and 2.64 ± 0.56 mm (width), with shoots reaching 15.67 ± 3.82 mm in height (Supplementary Table 2). Shoot density showed substantial spatial variation (255–39,852 shoots m^{-2}), averaging 17,844 ± 12,639 shoots m^{-2} across the meadow. Significant differences were observed among transects ($P < 0.01$, $F = 13.57$), with the lowest density at Y4 (7,639 ± 5,729 shoots m^{-2}) and the highest at Y3 (34,717 ± 6,432 shoots m^{-2}) (Table 2).

The carbon storage characteristics of *H. beccarii* showed significant spatial variation across the study area. Above-ground biomass C_{org} stocks averaged 1.22 ± 0.93 g C m^{-2}, exhibiting marked differences among transects ($P < 0.01$, $F = 10.39$). The values ranged from 0.17 ± 0.13 g C m^{-2} at transect Y5 to 2.27 ± 0.35 g C m^{-2} at transect Y3 (Complementary Table 2; Fig. 2a). Below-ground biomass displayed similar variability, with mean stocks of 1.12 ± 0.91 g C m^{-2} ($P < 0.05$, $F = 7.41$), reaching minimum (0.20 g C m^{-2} at Y6) and maximum (2.53 ± 0.47 g C m^{-2} at Y3) values. Total biomass C_{org} stocks demonstrated a 60-fold variation across transects, from 0.40 ± 0.33 g C m^{-2} at Y5 to 4.80 ± 0.30 g C m^{-2} at Y3. The above-to-

below-ground biomass ratio averaged 1.28 ± 0.88, with statistically significant differences among transects ($P < 0.01$, $F = 25.80$), indicating substantial spatial heterogeneity in biomass allocation patterns.

Figure 2

The total biomass carbon storage averaged 0.024 ± 0.018 Mg C ha^{-1}, corresponding to 10.03 ± 7.52 Mg C across the entire 418 ha meadow. Contrastingly, sediment carbon stocks (0–1 m depth) showed substantially higher values, averaging 82.13 ± 28.82 Mg C ha^{-1} (34,333 ± 12,049 Mg C) and ranging 33.57–125.29 Mg C ha^{-1}, with significant spatial variation among transects ($P < 0.001$, $F = 10.54$). Notably, transect Y5 contained the highest sediment stocks (114.57 ± 10.71 Mg C ha^{-1}), representing 2.36-fold greater storage than transect Y3 (48.52 ± 11.17 Mg C ha^{-1}). The combined carbon pool (biomass + sediment) totalled 34,343 ± 12,049 Mg C, with sediments accounting for > 99.99% of the stored carbon (Fig. 2b). The significant disparity highlights the predominant role of sediment carbon sequestration in the seagrass ecosystem, while living biomass insignificantly contributed to the total carbon storage.

3.2 Spatial variability analysis in sediment characteristics

The sediment characteristics exhibited pronounced spatial heterogeneity across the study area (Fig. 3). Moisture content averaged 29.00 ± 8.53% and ranged from 16.20–55.30%, with the minimum and maximum values at transects Y3 and Y7, respectively (Fig. 3a). Salinity displayed an average of 1.15 ± 0.53‰, varying between 0.37‰ and 2.75‰, where transect Y3 recorded the lowest mean salinity (0.77 ± 0.31‰) and Y7 the highest (2.08 ± 0.32‰) (Fig. 3b). The pH values averaged 7.72 ± 0.84, with transect Y3 exhibiting the lowest mean pH (7.29 ± 0.27), while Y1 (7.77 ± 0.23) and Y7 (7.75 ± 0.22) displayed the highest values (Fig. 3c). DBD ranged 0.36–2.13 g cm^{-3} (mean: 1.30 ± 0.39 g cm^{-3}), with the minimum at Y7 (0.94 ± 0.34 g cm^{-3}) and maximum at Y4 (1.59 ± 0.37 g cm^{-3}) (Fig. 3d).

C_{org} density varied considerably from 1.85 to 19.13 mg C cm^{-3} (mean: 8.07 ± 4.00 mg C cm^{-3}), peaking at Y7 (11.47 ± 3.38 mg cm^{-3}) and Y5 (10.29 ± 4.68 mg cm^{-3}), while reaching a minimum at Y3 (4.76 ± 3.20 mg C cm-3) and Y2 (5.10 ± 1.85 mg cm-3) (Fig. 3e). Organic carbon percentage ($\%C_{org}$) ranged 0.13–1.85% (mean: 0.67 ± 0.37%), with Y7 (1.29 ± 0.22%) and Y3 (0.39 ± 0.18%) representing the extremes (Fig. 3f). Additional parameters showed the following patterns: %LOI averaged 0.04 ± 0.02% (range: 0.01–0.10%; Fig. 3g); $\%CaCO_3$ ranged 0.50–3.92% (mean: 1.52 ± 0.80%), being lowest at Y3 (0.82 ± 0.28%) and highest at Y7 (3.97 ± 0.39%; Fig. 3h); and $\delta^{13}C$ varied between − 27.71‰ and − 22.65‰ (mean: -26.00 ± 1.50‰), with the most depleted values at Y5 and Y6 and the most enriched at Y1 (Fig. 3i).

Figure 3

The sediment characteristics exhibited distinct vertical variations across depth profiles (Fig. 4). Moisture content displayed a gradual decreasing trend with depth at transect Y7 (Fig. 4a). Salinity showed a

consistent reduction from 0 cm to 30 cm depth across all seven transects (Fig. 4b). DBD demonstrated a progressive increase from surface layers to 40 cm depth, with particularly notable increasing trends observed at transects Y1, Y3, and Y7 (Fig. 4d). %$CaCO_3$ exhibited a more complex vertical pattern, initially decreasing from 0 cm to 40 cm before increasing again between 50 cm and 100 cm at transects Y2, Y3, and Y5 (Fig. 4h). The remaining sediment parameters showed unclear or inconsistent vertical distribution patterns.

Figure 4

3.3 Analysis of driving factors that influence C_{org} stocks variations

Relationships between biomass C_{org} stocks and vegetation characteristics: biomass C_{org} stocks exhibited strong positive correlations with above-ground biomass C_{org} ($r = 0.97$, $p < 0.01$), shoot density ($r = 0.92$, $p < 0.01$), and below-ground biomass C_{org} ($r = 0.98$, $p < 0.01$). Additionally, significant positive associations were observed with shoot height ($r = 0.55$, $p < 0.05$) and leaf length ($r = 0.52$, $p < 0.05$) (Fig. 5a).

Negative correlations with sediment and blue carbon parameters: biomass C_{org} stocks showed significant inverse relationships with sediment C_{org} stocks ($r = -0.73$, $p < 0.01$), blue carbon storage ($r = -0.73$, $p < 0.01$), C_{org} density ($r = -0.74$, $p < 0.01$), %C_{org} ($r = -0.68$, $p < 0.01$), %LOI ($r = -0.67$, $p < 0.01$), and %$CaCO_3$ ($r = -0.55$, $p < 0.05$) (Fig. 5a).

Sediment %C_{org} relationships: sediment %C_{org} was negatively correlated with DBD ($r = -0.56$, $p < 0.01$). Conversely, sediment %C_{org} displayed strong positive correlations with sediment C_{org} stocks ($r = 0.78$, $p < 0.01$), blue carbon storage ($r = 0.78$, $p < 0.01$), C_{org} density ($r = 0.80$, $p < 0.01$), organic matter content ($r = 0.97$, $p < 0.01$), %$CaCO_3$ ($r = 0.92$, $p < 0.01$), salinity ($r = 0.89$, $p < 0.01$), and moisture content ($r = 0.92$, $p < 0.01$) (Fig. 5a, $N = 20$). Consistent patterns were observed across all sediment subsamples (Fig. 5b, $N = 140$).

Figure 5

Figure 6

Additionally, linear regression analysis also revealed significant positive correlations between %C_{org} and several environmental variables, including moisture content ($y = 0.036x + 0.364$, $R^2 = 0.69$), salinity ($y = 0.531x + 0.064$, $R^2 = 0.60$), $CaCO_3$ content ($y = 0.397x + 0.069$, $R^2 = 0.74$) and organic matter (%LOI, $y = 0.148x + 0.012$, $R^2 = 0.60$) (Fig. 6a, c, d, and f, respectively). A weaker but still significant negative correlation was observed between %C_{org} and DBD, $\delta^{13}C$, and shoot density (Fig. 6a, g, and h, respectively).

The first two principal components (PC1 and PC2) explained 78.65% of the total variance (PC1: 51.41%; PC2: 27.23%) (Fig. 7a, Supplementary Table 3). Both components were strongly associated with seagrass traits and sediment characteristics. PC1 displayed negative loadings for seagrass traits (e.g., coverage, biomass C_{org}, shoot density) but positive loadings for sediment characteristics, including moisture content, salinity, $\%CaCO_3$ content, %LOI, $\%C_{org}$, C_{org} density, and blue carbon storage. In contrast, PC2 was predominantly associated with positive loadings of the above-ground biomass C_{org}, leaf length, and shoot density, but negative loading for DBD. Similarly, for sediment characteristics alone, the first two PCs explained 78.50% of the total variance (PC1: 58.16%; PC2: 20.34%; Fig. 7b, Supplementary Table 3). PC1 also demonstrated significant influence from sediment properties, with negative loadings for DBD and $\delta^{13}C$, and positive loadings for sediment C_{org} density, $\%C_{org}$, salinity, $\%CaCO_3$, %LOI, and moisture content.

Figure 7

3.4 Sediment C_{org} sources at different transects

The sediment sub-samples exhibited an average $\delta^{13}C$ value of -26.00 ± 1.50‰. The Bayesian mixing model results of $\delta^{13}C$ showed that the C_{org} of the upper 1 m sediment mainly originated from terrigenous C_{org} (49.84 ± 23.57%), seagrass C_{org} (26.83 ± 21.43%), and phytoplankton C_{org} (23.33 ± 19.98%) (Supplementary Table 4). Vertical distributions of C_{org} sources displayed opposing trends: terrigenous inputs dominated at depth (53.10 ± 23.00% at 50–70 cm) but decreased by approximately 7% toward surface layers (46.00 ± 20.00% at 0–10 cm). Seagrass C_{org} (24.90 ± 18.50% to 28.90 ± 20.40%) and phytoplankton C_{org} (22.0 ± 18.5% to 25.10 ± 18.40%) showed proportional increases in surface sediments (Fig. 8a). Sediment C_{org} sources also exhibited distinct spatial variation along the transect, with seagrass- and phytoplankton-derived C_{org} decreasing and terrigenous C_{org} increasing from Y1 to Y7 (Fig. 8b).

Figure 8

4. Discussion

4.1 Comparison of blue carbon storage among different seagrass meadows

The living biomass carbon stock (0.028 ± 0.017 Mg C ha^{-1}) in the Yifengxi Estuary's *H. beccarii* meadow represents only 1.1% of the global seagrass average (2.52 ± 0.48 Mg C ha^{-1}), though it falls within the documented range for this species (0.001–5.54 Mg C ha^{-1})[7]. The biomass C_{org} stock was evidently influenced by the seagrass characteristics, e.g. shoot density, shoot height, and leaf length. This limited biomass accumulation reflects *H. beccarii*'s ecological strategy as a pioneer species—its small morphological structure, coupled with rapid growth rates and high turnover, facilitates efficient organic

matter decomposition in sediments[29,47], contrasting with the greater carbon retention in larger, longer-lived seagrass species.

Sediment carbon stocks (0–1 m depth) in the study area measured 82.13 ± 28.82 Mg C ha⁻¹, comparable to *H. beccarii* meadows at similar latitudes in Guangxi, China (83.98 Mg C ha⁻¹)[48]. However, these values are substantially lower than both the global median (139.7 Mg C ha⁻¹) and mean (194.2 Mg C ha⁻¹) for seagrass ecosystems[7]. Regional comparisons further highlight this disparity, with *H. beccarii* meadows in Singapore (138 ± 8.6 Mg C ha⁻¹)[49] and Beibu Gulf, Guangxi (112 ± 33.3 Mg C ha⁻¹, obtained by extrapolating from the carbon storage data ranging 0–60 cm)[50] demonstrating 68–37% greater carbon storage capacity. The blue carbon storage capacity of *H. beccarii* meadows was comparatively lower than other dominant seagrass genera, including *Zostera* (mean: 108.9 Mg C ha⁻¹) and *Posidonia* (mean: 155 Mg C ha⁻¹)[20], but higher than Halophila ovalis in Liusha Bay (64.93 ± 22.31 Mg C ha^{-1}) in the coastal area of south China's Zhanjiang City[9]. This disparity reflects fundamental differences in carbon sequestration efficiency among seagrass species, which scales positively with both morphological characteristics (e.g., leaf size and canopy structure) and habitat-forming capacity (e.g., habitat configuration in bay, estuarine, or open-water environments)[48,51].

4.2 Key factors affecting the variability of sediment C_{org} stocks

The spatial distribution of sediment C_{org} stocks in seagrass meadows is governed by a complex interplay of biotic and abiotic factors, including seagrass species traits, topographic features, hydrodynamic conditions, water depth, and sediment physicochemical properties[23,27]. Synergistic interactions among these environmental variables can significantly enhance the carbon sequestration capacity of seagrass ecosystems[20]. Generally, larger-bodied seagrass species with more extensive canopies and high shoot density demonstrate enhanced sediment trapping efficiency, facilitating greater accumulation of allochthonous carbon inputs. This relationship likely stems from two key mechanisms: (1) taller canopy structure associated with higher aboveground biomass reduces near-bed flow velocities, and (2) greater three-dimensional habitat complexity enhances particle trapping efficiency, thereby increasing the deposition of suspended organic matter[51]. However, the shoot density and biomass C_{org} stocks showed significant inverse relationships with sediment C_{org} stocks in the study (Figs. 2 and 5a). This suggests that the sediment characteristics, along with other key factors (e.g., topographic features, hydrodynamic conditions, discharge and tide flow), are critical determinants of the spatial distribution patterns of C_{org} stocks.

The sediment $\%C_{org}$ and C_{org} density exhibited significant positive correlations with moisture, salinity, and $CaCO_3$ content, and a significant negative correlation with DBD, indicating their synergistic role in promoting long-term carbon sequestration. These factors enhance C_{org} storage through key mechanisms below.

Moisture-Oxygen Dynamics: High moisture content was associated with reduced oxygen permeability due to its close relationship with DBD and sediment grain size[8]. The resulting hypoxic conditions suppressed organic matter decomposition[52,53], thereby promoting C_{org} accumulation.

Salinity-Microbial Regulation

Elevated salinity reduced microbial biomass and extracellular enzyme activity[54], limiting organic matter microbial mineralisation. This salinity-induced suppression of degradation further contributed to higher sedimentary C_{org} retention.

Carbonate-Associated Preservation: $CaCO_3$ adsorption physically protected C_{org} from oxidation while restricting microbial access, synergistically enhancing long-term storage through two key processes: (1) physical protection of organic matter through adsorption and (2) reduced exposure to oxidative degradation, thereby decreasing mineralisation rates[55]. This carbonate-mediated preservation mechanism is further supported by Ingalls et al. (2004)[56], who identified that $CaCO_3$ matrices provide both intra- and inter-crystalline spaces for organic matter storage, while surface adsorption creates a protective barrier that limits microbial access and subsequent oxidation of C_{org}. Arina et al. (2020)[57] also found that $CaCO_3$ deposition by calcifying algae in disturbed seagrass beds enhances organic carbon stabilisation for long-term storage.

The inverse relationship between DBD and $\%C_{org}$ may reflect a dynamic equilibrium among three key factors: organic matter input, sediment physical structure, and microbial decomposition. High organic matter input from sources like dense vegetation can reduce DBD (e.g., the lowest DBD, the highest $\%C_{org}$, and 55% terrigenous C_{org} source at transect Y7) by increasing sediment porosity, while the resulting low-density, high-porosity structure in turn protects C_{org} by limiting oxygen diffusion and suppressing microbial mineralisation[58]. This self-reinforcing mechanism creates a positive feedback loop that sustains elevated C_{org} stocks in low-DBD sediments in seagrass meadows.

Estuarine ecosystems serve as critical zones for processing, transporting, and sequestering terrestrial and marine-derived organic matter[59]. The sediment C_{org} source order was terrigenous C_{org} >seagrass C_{org} >phytoplankton C_{org} in the *H. beccarii* seagrass meadow (Fig. 8a). As terrigenous C_{org} usually has higher C_{org} content and low $\delta^{13}C$ (due to the presence of recalcitrant lignin), its reduction will lead to a decrease in the total $\%C_{org}$ and an increase in $\delta^{13}C$[60,61]. The distinct spatial variation occurred along the transect, with seagrass- and phytoplankton-derived C_{org} decreasing and terrigenous C_{org} increasing from Y1 to Y7 (Fig. 8a). A significant negative correlation was also observed between $\%C_{org}$ and $\delta^{13}C$ (Fig. 6g). Therefore, the sediment C_{org} source can influence sediment C_{org} stocks variation. Additionally, for the Yifengxi Estuary, characterised by a low flow rate, the mid-reach of the river mouth (transects Y4 to Y7) exhibits a more favourable geomorphological setting for the accumulation of terrestrial organic matter, with terrigenous C_{org} content exceeding 55%. This depositional hotspot likely results from the

interplay of reduced hydrodynamic energy, localised topographic traps, and proximity to terrestrial organic inputs (e.g., mangroves).

These findings suggest that targeted management of environmental parameters (e.g., sediment composition through substrate amendments) could potentially optimise the carbon storage function of seagrass meadows as a nature-based climate solution. The substantial variability in carbon stocks observed even within the same genus highlights the importance of site-specific combinations of environmental characteristics, including salinity gradients, sediment moisture, $CaCO_3$ content, and DBD, in determining ultimate sequestration capacity. Further analysis can include long-term monitoring to assess seasonal and interannual C_{org} dynamics and comparative studies with other seagrass species to broaden the study findings.

5. Conclusions

Our study investigated the spatial variation of blue carbon storage and the sources of sedimentary C_{org} in *H. beccarii* seagrass meadows, using multi-site sampling and stable isotope analysis. Focusing on the Yifengxi Estuary in a subtropical monsoon climate zone—where reliable blue carbon data for seagrass ecosystems remain scarce—both the biological and sedimentary carbon stocks were quantified. The study results revealed a relatively low living biomass carbon stock (0.028 ± 0.017 Mg C ha^{-1}), consistent with *H. beccarii*'s pioneer species characteristics, and a substantial sediment carbon stock (82.41 ± 29.99 Mg C ha^{-1} in the upper 1 m), demonstrating significant below-ground sequestration potential. Key environmental drivers of C_{org} preservation included high moisture content and elevated salinity, which reduced sediment oxygen permeability and microbial activity and $CaCO_3$ enrichment, which enhanced C_{org} adsorption and physical protection from mineralisation. High organic matter input from terrigenous sources like dense vegetation reduces DBD by increasing sediment porosity, while the resulting low-density, high-porosity structure in turn protects C_{org} by limiting oxygen diffusion and suppressing microbial mineralization. These factors collectively created reducing conditions that suppressed extracellular enzyme activity and microbial degradation rates, thereby promoting long-term carbon storage. Terrigenous sources contributed most sediment carbon (49.84 ± 23.57%), followed by seagrass (26.83 ± 21.43%), and phytoplankton (23.33 ± 19.98%), exhibiting distinct spatial variation along the transect. The study findings provide critical baseline data for blue carbon assessments in understudied subtropical monsoon regions and recommend that targeted management of environmental parameters could potentially optimise the carbon storage function of seagrass meadows as a nature-based climate solution.

Declarations

Acknowledgement

This work was financially supported by the Guangdong Basic and Applied Basic Research Foundation (2025A1515012007), National Natural Science Foundation of China (42071030 and 52379067) and Nansha Key Scientific and Technological Project, Guangdong Province (2023ZD012). We would like to thank Editage (www.editage.com) for English language editing.

References

1. CO_2 Earth, 2025. https://www.co2.earth/earths-CO2-main-page.
2. Gouldsmith, V. & Cooper, A. Consideration of the carbon sequestration potential of seagrass to inform recovery and restoration projects within the Essex Estuaries Special Area of Conservation (SAC), United Kingdom. *J. Coast. Conserv.* 26, 36 (2022).
3. Schaefer, R., Colarusso, P., Simpson, J. C., Novak, A. & Nepf, H. Continual migration of patches within a Massachusetts seagrass meadow limits carbon accretion and storage. *Commun Earth Environ.* 6, 129 (2025).
4. Himes-Cornell, A., Pendleton, L. & Atiyah, P. Valuing ecosystem services from blue forests: A systematic review of the valuation of salt marshes, sea grass beds and mangrove forests. *Ecosyst. Serv.* 30, 36–48 (2018).
5. Macreadie, P. I., Baird, M. E., Trevathan-Tackett, S. M., Larkum, A. W. D. & Ralph, P. J. Quantifying and modelling the carbon sequestration capacity of seagrass meadows – A critical assessment. *Mar. Pollut. Bull.* 83, 430–439 (2014).
6. Potouroglou, M. et al. The sediment carbon stocks of intertidal seagrass meadows in Scotland. *Estuar. Coast. Shelf Sci.* 258, 107442 (2021).
7. Fourqurean, J. W. et al. Seagrass ecosystems as a globally significant carbon stock. *Nat. Geosci.* 5, 505–509 (2012).
8. Kim, S. H. et al. Variability in blue carbon storage related to biogeochemical factors in seagrass meadows off the coast of the Korean peninsula. *Sci. Total Environ.* 813, 152680 (2022).
9. Shen, X. et al. Spatial variability in blue carbon storage and sequestration of seagrass meadows in southern China. *Sci. Total Environ.* 951, 175884 (2024).
10. Smith, S. V. Marine Macrophytes as a Global Carbon Sink. *Science* 211, 838–840 (1981).
11. Huang, Y-H., Lee, C-L., Chung, C-Y., Hsiao, S-C. & Lin H-J. Carbon budgets of multispecies seagrass meadows at Dongsha Island in the South China Sea. *Mar. Environ. Res.*106, 92–102 (2015).
12. Rozaimi M, Lavery P S, Serrano O. & Krywood, D. Long-term carbon storage and its recent loss in an estuarine Posidonia australis meadow (Albany, Western Australia). *Estuar. Coast. Shelf Sci.* 171, 58–65 (2016).
13. Jiang, Z. et al. Newly discovered seagrass meadows and their potential for blue carbon in the coastal seas of Hainan Island, South China Sea. *Mar. Pollut. Bull.* 125, 513–521 (2017).
14. Serrano, O., Almahasheer, H., Duarte, C. M. & Irigoien, X. Carbon stocks and accumulation rates in Red Sea seagrass meadows. *Sci Rep* 8, 15037 (2018).

15. Wahyudi, A. J. et al. Assessing Carbon Stock and Sequestration of the Tropical Seagrass Meadows in Indonesia. *Ocean Science Journal* 55, 85–97 (2020).
16. Stankovic, M. et al. Blue carbon assessments of seagrass and mangrove ecosystems in South and Southeast Asia: Current progress and knowledge gaps. 904, 166618 (2023).
17. Serrano, O., Lavery, P. S., Rozaimi, M. & Mateo, M. A. Influence of water depth on the carbon sequestration capacity of seagrasses. *Glob. Biogeochem. Cycles* 28, 950–961 (2014).
18. Alongi, D. M. et al. Indonesia's blue carbon: a globally significant and vulnerable sink for seagrass and mangrove carbon. *Wetl. Ecol. Manag.* 24, 3–13 (2016).
19. Ricart, A. M. et al. High variability of Blue Carbon storage in seagrass meadows at the estuary scale. *Sci Rep* 10, 5865 (2020).
20. Röhr, M. E. et al. Blue Carbon Storage Capacity of Temperate Eelgrass (Zostera marina) Meadows. *Glob. Biogeochem. Cycles* 32, 1457–1475 (2018).
21. Belshe, E. F., Hoeijmakers, D., Herran, N., Mtolera, M. & Teichberg, M. Seagrass community-level controls over organic carbon storage are constrained by geophysical attributes within meadows of Zanzibar, Tanzania. *Biogeosciences* 15, 4609–4626 (2018).
22. Su, Z., Qiu, G., Fan, H. & Fang, C. 2020. Seagrass beds store less carbon but support more macrobenthos than mangrove forests. *Mar. Environ. Res.* 162, 105162 (2020).
23. Mazarrasa, I. et al. Habitat characteristics provide insights of carbon storage in seagrass meadows. *Mar. Pollut. Bull.* 134, 106–117 (2018).
24. Singh, S., Lal, M. M., Southgate, P. C., Wairui, M. & Singh, A. Blue carbon storage in Fijian seagrass meadows: First insights into carbon, nitrogen and phosphorus content from a tropical southwest Pacific Island. *Mar. Pollut. Bull.* 176, 113432 (2022).
25. Bijak, A. L., Reynolds, L. K.& Smyth, A. R. Seagrass meadow stability and composition influence carbon storage. *Landscape Ecol.* 38, 4419–4437 (2023).
26. Lei, J., et al. Spatial heterogeneity in sediment and carbon accretion rates within a seagrass meadow correlated with the hydrodynamic intensity. *Sci. Total Environ.* 8548, 158685 (2023).
27. Samper-Villarreal, J., Lovelock, C. E., Saunders, M. I., Roelfsema, C. & Mumby, P. J. Organic carbon in seagrass sediments is influenced by seagrass canopy complexity, turbidity, wave height, and water depth. *Limnol. Oceanogr.* 61, 938–952 (2016).
28. Kennedy, H., et al. (2022) Species traits and geomorphic setting as drivers of global soil carbon stocks in seagrass meadows[J]. *Global Biogeochem. Cycles* 36(10), 1–18.
29. Serrano, O. et al. Can mud (silt and clay) concentration be used to predict soil organic carbon content within seagrass ecosystems?. *Biogeosciences* 13, 4915–4926 (2016).
30. Mazarrasa, I. et al. Factors determining seagrass blue carbon across bioregions and geomorphologies. *Global Biogeochem. Cycles* 35, 1–17 (2021).
31. Asplund, M. E. et al. Dynamics and fate of blue carbon in a mangrove-seagrass seascape: influence of landscape configuration and land-use change[J]. *Landscape Ecol.* 36, 1489–1509 (2021).

32. Lavery, P. S., Mcmahon, K., Weyers, J., Boyce, M. C., & Oldham, C. E. Release of dissolved organic carbon from seagrass wrack and its implications for trophic connectivity[J]. *Mar. Ecol. Prog. Ser.* 494(3), 121–133 (2013).
33. Spivak, A. C., Sanderman, J., Bowen, J. L., Canuel, E. A. & Hopkinson, C. S. Global-change controls on soil-carbon accumulation and loss in coastal vegetated ecosystems. *Nat. Geosci.* 12, 685–692 (2019).
34. Novak, A. B. et al. Factors Influencing Carbon Stocks and Accumulation Rates in Eelgrass Meadows Across New England, USA. *Estuaries Coasts* 43, 2076–2091 (2020).
35. Alemu, I. J. B. et al. Geomorphic gradients in shallow seagrass carbon stocks. *Estuar. Coast. Shelf Sci.* 265, 107681 (2022).
36. Jiang, Z. et al. Historical changes in seagrass meadows in a rapidly urbanizing area of Guangdong Province: Implications for conservation and management. *Glob. Ecol. Conserv.* 22, e01035 (2020).
37. Zhou, Y. et al. Distribution status, degradation reasons and protection countermeasures of seagrass resources in China. *Oceanol. Limnol. Sin.* 54, 1248–1257 (2023). (In Chinese)
38. Short, F. T. et al. Extinction risk assessment of the world's seagrass species. *Biol. Conserv.* 144, 1961–1971 (2011).
39. Howard, J., Hoyt, S., Isensee, K., et al. Coastal blue carbon: methods for assessing carbon stocks and emissions factors in mangroves, tidal salt marshes, and seagrasses, International Union for Conservation of Nature (IUCN): Arlington, VA, USA (2014).
40. Duarte, C. M. Seagrass nutrient content. *Mar. Ecol. Prog. Ser.* 67, 201–207 (1990).
41. Chen, L., Lu, W. & Lin, G. (translation). Methods for assessing carbon stocks and carbon emission factors in coastal blue carbon mangrove, salt marsh and seagrass meadows (M). (eds Howard, J., Hoyt, S., Isensee, K., Pidgeon, E. & Telszewski, M.) (2018). (In Chinese)
42. Heiri, O., Lotter, A. F. & Lemcke, G. Loss on ignition as a method for estimating organic and carbonate content in sediments: reproducibility and comparability of results. *J. Paleolimnol.* 25, 101–110 (2001).
43. Bengtsson, L. & Enell, M. Chemical analysis. In *Handbook of Holocene Palaeoecology and Palaeohydrology* (ed Berglund, B. E.) 423–451 (John Wiley & Sons Ldt., Chichester, 1986).
44. Stock, B. C. et al. Analyzing mixing systems using a new generation of Bayesian tracer mixing models. *PeerJ* 6, e5096 (2018).
45. Kennedy, H. et al. Seagrass sediments as a global carbon sink: Isotopic constraints. *Glob. Biogeochem. Cycles* 24, GB4026 (2010).
46. Hou W, Gu B, Lin Q, Gu, J. & Han, B-P. Stable isotope composition of suspended particulate organic matter in twenty reservoirs from Guangdong, southern China: Implications for pelagic carbon and nitrogen cycling. *Water Res*. 47, 3610–3623 (2013).
47. Kilminster, K. et al. 2015. Unravelling complexity in seagrass systems for management: Australia as a microcosm. *Sci. Total Environ.* 534, 97–109 (2015).

48. Li, M. Carbon storage in the seagrass sediments of Guangxi, China. Guangxi Normal University (2018). (In Chinese).
49. Phang, V. X. H., Chou, L. M. & Friess, D. A. Ecosystem carbon stocks across a tropical intertidal habitat mosaic of mangrove forest, seagrass meadow, mudflat and sandbar. *Earth Surf. Process. Landf.* 40, 1387–1400 (2015).
50. Su, Z.N., Qiu, G. L., Fan, H. Q. & Fang, C. Seagrass beds store less carbon but support more macrobenthos than mangrove forests. *Mar Environ Res* 162, (2020).
51. Fonseca, M. S. & Cahalan, J. A. A preliminary evaluation of wave attenuation by four species of seagrass. *Estuar. Coast. Shelf Sci.* 35, 565–576 (1992).
52. Kroeger, K. D., Crooks, S., Moseman-Valtierra, S. & Tang, J. Restoring tides to reduce methane emissions in impounded wetlands: A new and potent Blue Carbon climate change intervention. *Sci Rep* 7, 11914 (2017).
53. Zhao, Q. et al. Soil organic carbon content and stock in wetlands with different hydrologic conditions in the Yellow River Delta, China. *Ecohydrol. Hydrobiol.* 20, 537–547 (2020).
54. Rath, K. M. & Rousk, J. Salt effects on the soil microbial decomposer community and their role in organic carbon cycling: A review. *Soil Biol. Biochem.* 81, 108–123 (2015).
55. Mazarrasa, I. et al. Seagrass meadows as a globally significant carbonate reservoir. *Biogeosciences* 12, 4993–5003 (2015).
56. Ingalls, A. E., Aller, R. C., Lee, C. & Wakeham, S. G. Organic matter diagenesis in shallow water carbonate sediments. *Geochim. Cosmochim. Acta* 68, 4363–4379 (2004).
57. Arina, N. et al. Coralline macroalgae contribution to ecological services of carbon storage in a disturbed seagrass meadow. *Mar. Environ. Res.* 162, 105156 (2020).
58. Dahl, M. et al. Sediment properties as important predictors of carbon storage in *Zostera marina* meadows: a comparison of four European areas. *PLoS ONE* 11, e0167493 (2016).
59. Fu, C. et al. Substantial blue carbon sequestration in the world's largest seagrass meadow. *Commun. Earth Environ*. 4:474 (2023).
60. Tesi, T. et al. Composition and fate of terrigenous organic matter along the Arctic land-ocean continuum in East Siberia: insights from biomarkers and carbon isotopes. *Geochim. Cosmochim. Acta.* 133, 235–256 (2014).
61. Wu S, Liu J, Chu H, et al. 2025. Sources and influencing mechanisms of organic carbon in the western Bohai Sea over the past century. *Mar. Geol. Quat. Geol.* 45, 1–17 (2025). (In Chinese)

Figures

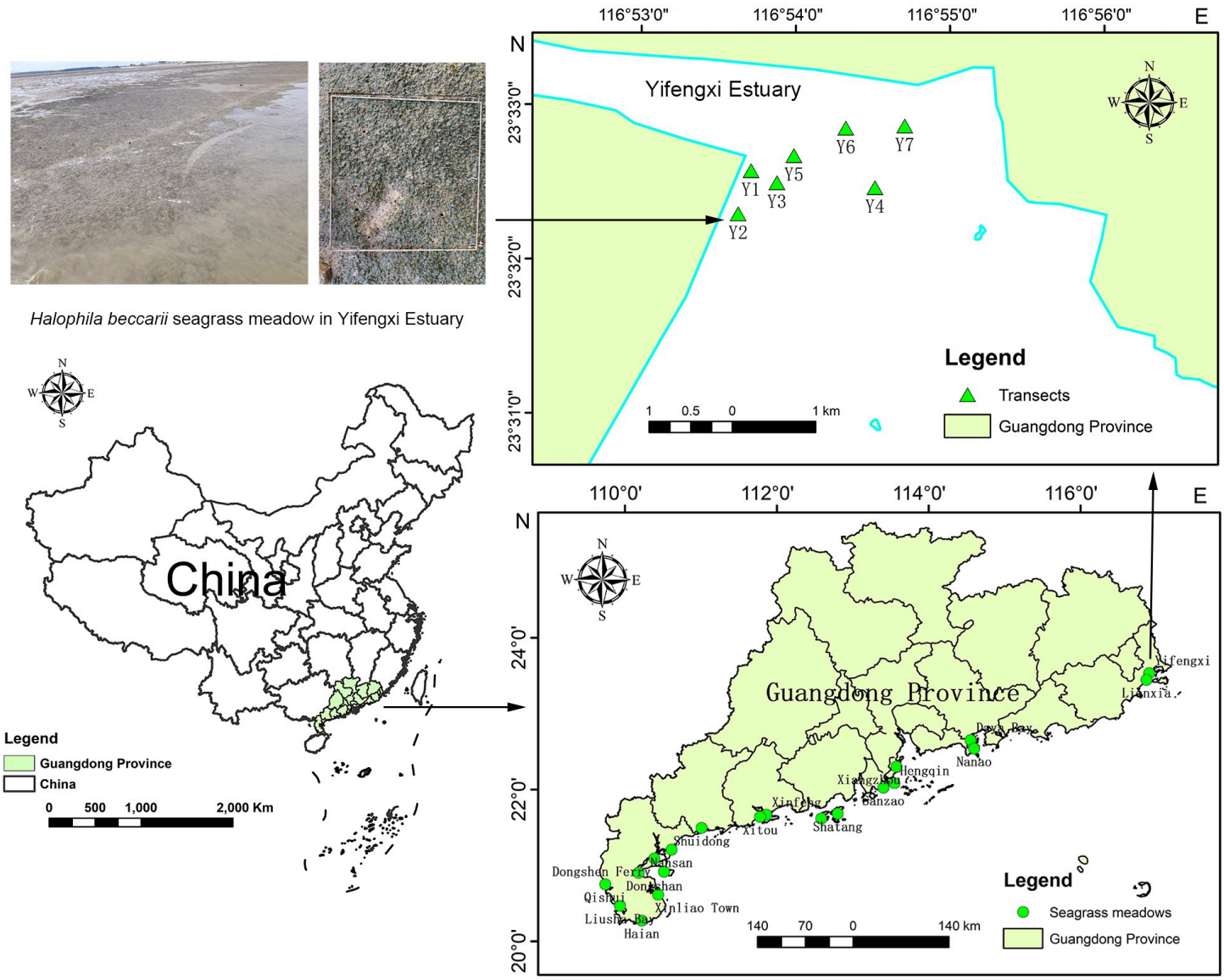

Figure 1

The location of seven sampling transects at the *Halophila beccarii* seagrass meadow in Yifengxi Estuary of Guangdong Province, southern China.

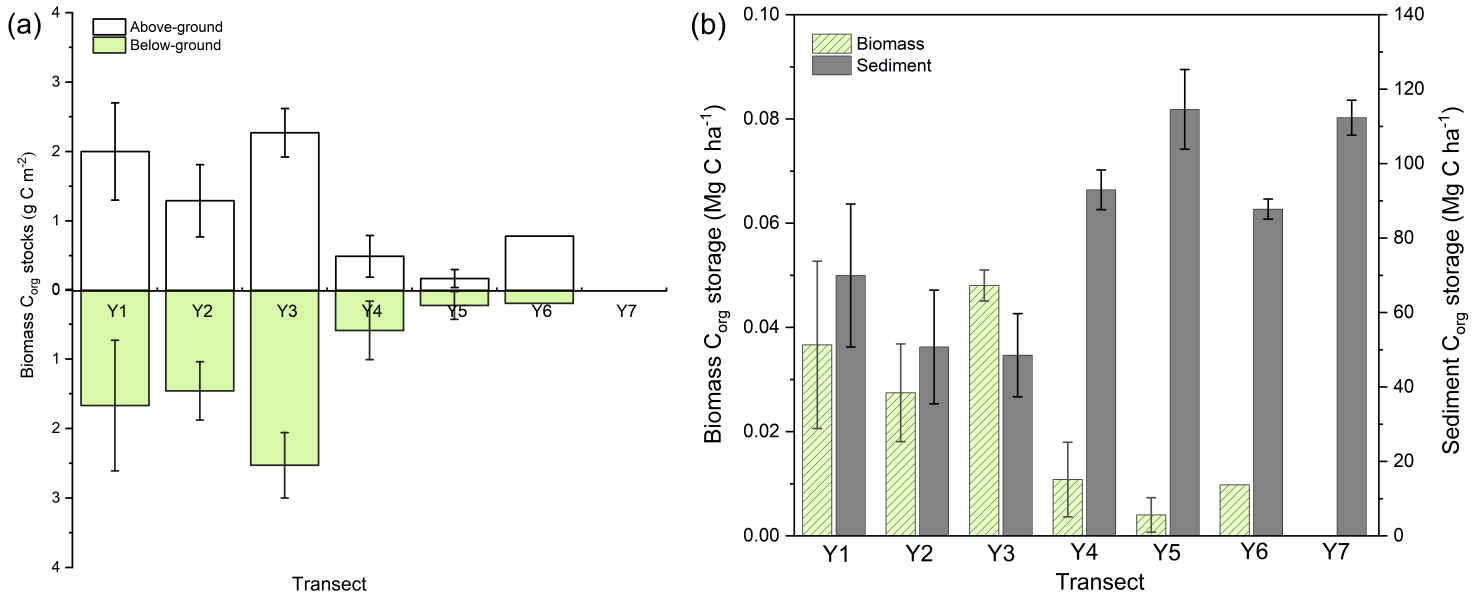

Figure 2

Halophila beccarii (*H. beccarii)* carbon storage characteristics. a) Spatial variation in above- and below-ground biomass C_{org} stocks at monitoring transects of *H. beccarii* seagrass meadows; b) total biomass and sediment C_{org} stocks of the upper 1 m at each transect.

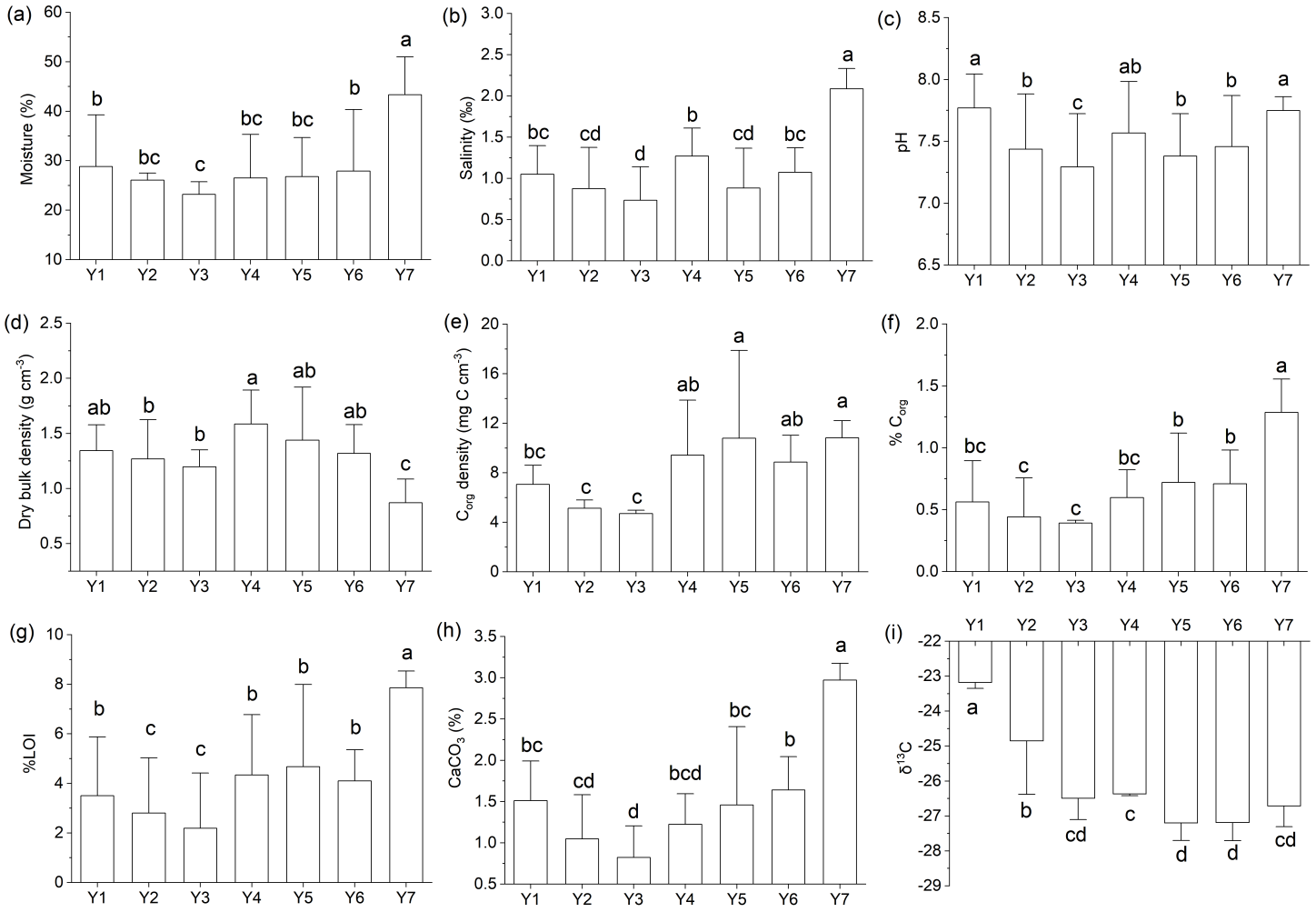

Figure 3

Spatial variability in sediment environmental characteristics and C_{org} at monitoring transects. a) Moisture; b) Salinity; c) pH; d) Dry bulk density; e) C_{org} density; f) C_{org}; g) Loss on ignition (LOI); h) $CaCO_3$; and i) $\delta^{13}C$. Different letters indicate significant differences at $p<0.05$.

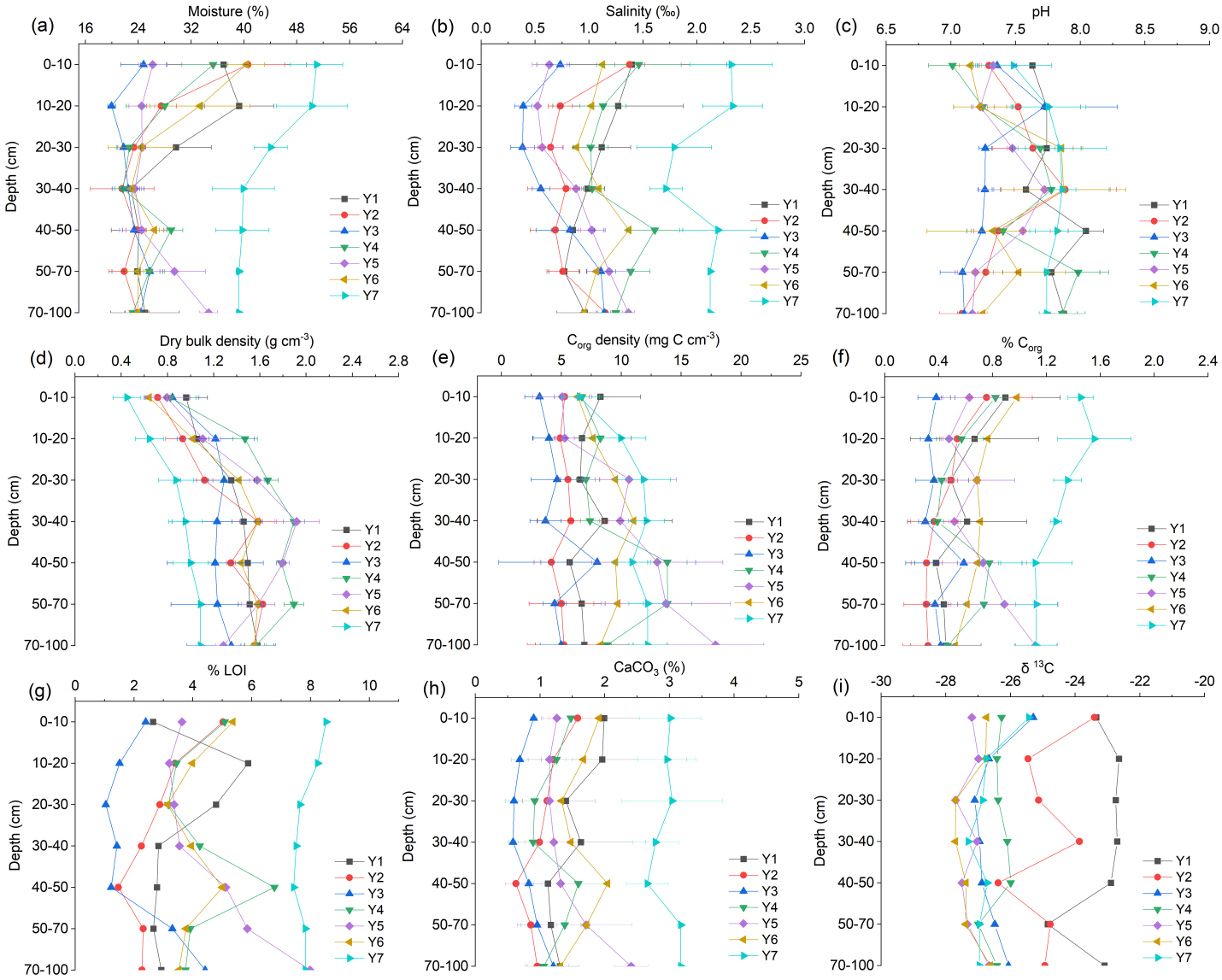

Figure 4

Vertical variations of the sediment characteristics across depth profiles. a) Moisture; b) Salinity; c) pH; d) Dry bulk density; e) C_{org} density; f) C_{org}; g) LOI; h) $CaCO_3$; and i) $\delta^{13}C$.

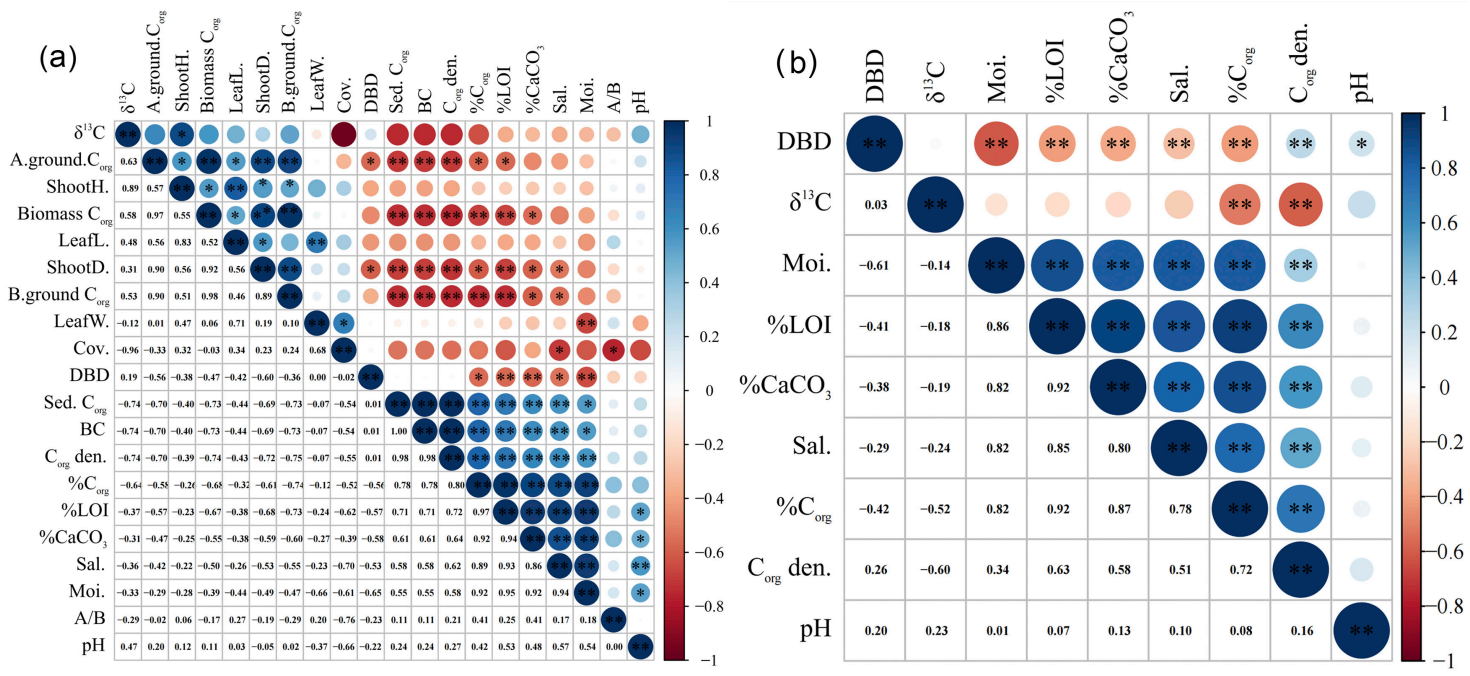

Figure 5

Correlation diagrams illustrating the relationship between biological characteristics, living biomass, biomass C_{org} stocks, sediment characteristics, and sediment C_{org} stocks in *H. beccarii* seagrass meadow. a) *N* = 20 and b) *N* = 140.

Abbreviations: Above-ground biomass C_{org} (A.ground.C_{org}), Below-ground biomass C_{org} (B.ground C_{org}), Aboveground-to-belowground biomass ratio of seagrass (A/B), Shoot height (ShootH.), Leaf length (LeafL.), Shoots density (ShootD.), Leaf width (LeafW.), Coverage (Cov.), dry bulk density (DBD), sediment C_{org} stock (Sed. C_{org}), blue carbon storage of biomass and sediment (BC), sediment C_{org} density (C_{org} den.), sediment organic carbon content (%C_{org}), organic matter content (%LOI), $CaCO_3$ content (%$CaCO_3$), salinity (Sal.), and moisture content (Moi.)

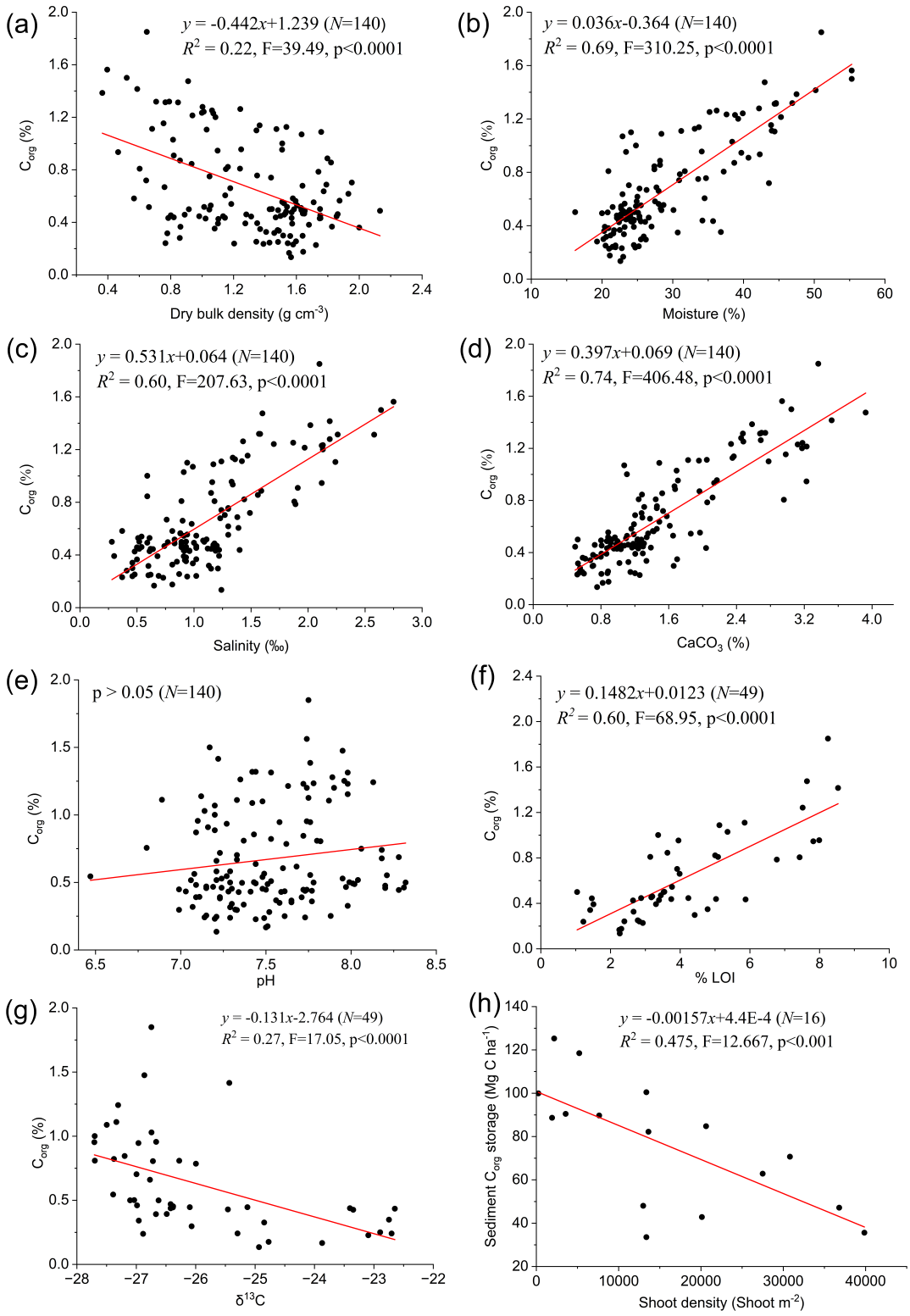

Figure 6

Linear regression analysis of sediment characteristics a) Dry bulk density; b) Moisture; c) Salinity; d) $CaCO_3$; e) pH; f) LOI; g) $\delta^{13}C$; and h) shoot density of seagrass.

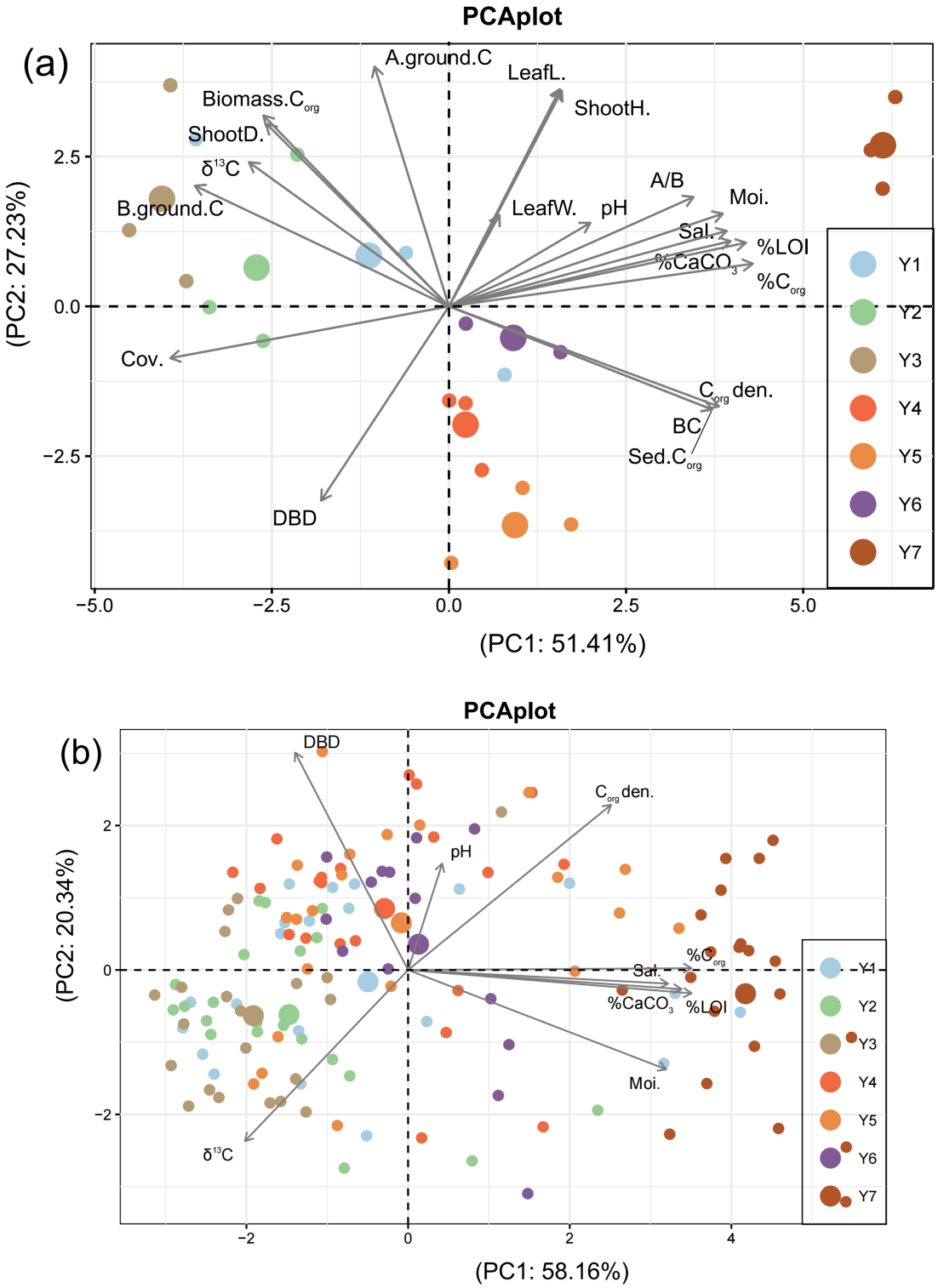

Figure 7

Principal component analysis (PCA) results. PCA among seagrass characteristics, sediment characteristics, and C_{org} density at *H. beccarii* seagrass meadow (a), $N = 20$) and PCA among sediment characteristics and C_{org} density (b), $N = 140$). Refer to Figure 5 for abbreviations.

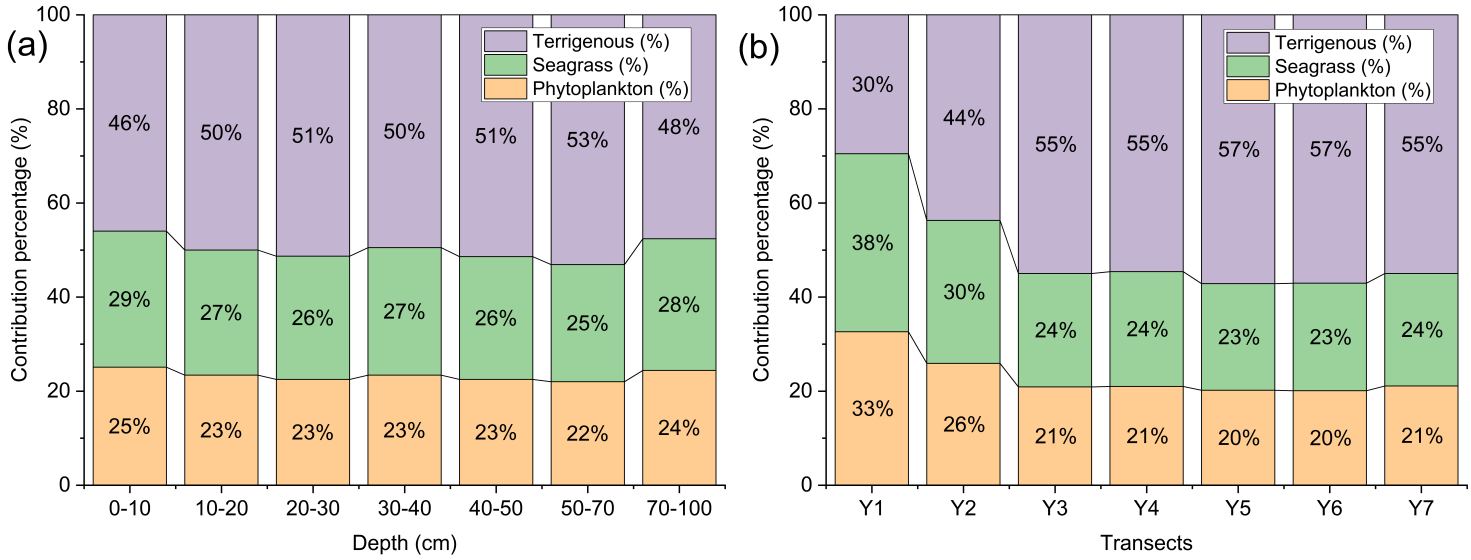

Figure 8

Relative contribution (%) of source to sediment C_{org} across seven transects. a) Depth profiles and b) Transects.

Supplementary Files

This is a list of supplementary files associated with this preprint. Click to download.

- SubSupplementaryTables.docx